Luminescence studies of optically pumped quantum wells in GaAs-$Al_xGa_{1-x}As$ multilayer structures

R. C. Miller, D. A. Kleinman, W. A. Nordland, Jr., and A. C. Gossard
Bell Laboratories, Murray Hill, New Jersey 07974
(Received 9 January 1980)

Various properties derivable from the photoluminescence of a multilayer structure consisting of many thin GaAs layers (wells) separated by thin $Al_xGa_{1-x}As$ layers (barriers) have been determined as a function of temperature from 7 K to greater than 150 K. These measurements, which were made utilizing both fixed- and tunable-frequency laser sources, include the following: the circular photoluminescence polarization ρ generated by circularly polarized optical excitation, the magnetic field dependence of ρ in the Voigt geometry (Hanle effect) to determine the electron lifetime τ and spin-relaxation time τ_s, the excitation spectrum for the peak of the photoluminescence which shows thirteen exciton quantum transitions characteristic of multilayer samples, the photoluminescence spectra which exhibit five transitions in emission, the excitation intensity I_p dependence of the integrated photoluminescence intensity, and τ and τ_s as a function of I_p. The temperature dependence of τ_s suggests that there is a center with a binding energy of about 5 meV that relaxes the electron spins at low temperatures. In the high-temperature region, $T \gtrsim 100$ K, τ_s is close to that observed by others for lightly doped p-type bulk GaAs and is close to estimates of τ_s for the D'yakonov-Perel' spin-relaxation mechanism. The absence of optical alignment with linearly polarized pumping and the characteristics of the magnetic field dependence of ρ both argue against significant hole polarization. The linear dependence of the integrated photoluminescence intensity on I_p leads to a simple model for the radiative lifetime whose temperature dependence is found to be consistent with expectations. Also, these data are used to estimate the nonradiative lifetime $\tau_n = 5 \times 10^{-9}$ sec which varies little with T and the radiative lifetime $\tau_r(T) = 3 \times 10^{-10}$ sec at 7 K, which varies $\sim T^{3/2}$.

INTRODUCTION

Although the quantum nature of multilayer structures consisting of many thin GaAs wells separated by thin AlGaAs barriers has been well documented,[1,2] few details and characteristics of the photoluminescence of such structures have been described. A recent study[3] of radiative recombination in such structures emphasizes the important role of free excitons. In the present work, various properties of a multilayer structure derivable from photoluminescence studies have been obtained as a function of temperature. These studies include: circular polarized photoluminescence along with the Hanle effect to determine the electron lifetime τ and the electron-spin-relaxation time τ_s,[2,4] the photoluminescence spectrum, the integrated photoluminescence intensity, and its pump power dependence. Some of the data are interpreted in terms of a simple recombination model which is used to estimate the temperature dependence and magnitude of the radiative and nonradiative lifetimes. Other aspects of the data shed light on the spin-relaxation mechanisms in these structures. The τ_s data suggest that there is a shallow center, ~5 meV deep, that relaxes the electron spin at low temperatures. In the high-temperature region τ_s is probably determined by the D'yakonov-Perel' process.[5] The magnetic field dependence of the circular photoluminescence and the absence of optical alignment[6] argue against hole polarization in the multilayer structures studied under the conditions of the present experiments.

The samples chosen for discussion here are believed to be particularly suitable for fundamental studies of photoluminescence because of their unusually high photoluminescence intensity coupled with a photoluminescence behavior that can be understood on the basis of simple and reasonable models. The results obtained are therefore believed to be appropriate to relatively pure, strain free, uniform, geometrically nearly perfect multilayer samples.

EXPERIMENTAL

The major portion of the data was obtained with a wafer grown by molecular beam epitaxy (MBE) that consisted of the following: a GaAs substrate with a (100) growth surface, 1 μm of $Al_{0.28}Ga_{0.72}As$, 30 periods of 260-Å wide GaAs wells and 260-Å wide $Al_{0.28}Ga_{0.72}As$ barriers, and finally, 1 μm of $Al_{0.28}Ga_{0.72}As$. The layers were not intentionally doped, which for bulk GaAs grown in this apparatus means p-type ~10^{14} cm^{-3}. The barriers are sufficiently wide so that tunneling effects[1] are insignificant for this study.

For excitation two different laser sources were utilized, a cw Kr^+ laser at 1.647 eV (7525 Å) and a pulsed tunable optical parametric oscillator (OPO). The incident light was normal to the plane of the layers and focused to a spot ~200 μm in diameter.

The generated luminescence, detected in the backward direction 24° off normal incidence, was passed through a circular polarization analyzer ($\lambda/4$ plate plus linear polarizer) before entering a $\frac{1}{2}$-m monochromator equipped with a cooled photomultiplier. The instrumental resolution was sufficiently high so as not to influence the results presented herein.

With the Kr^+ source the linearly polarized beam from the laser was chopped mechanically with $\lambda/4$ plates to yield + and − circular polarizations at 480 Hz. The photoluminescence signal I_{PL} at 240 Hz was ratioed with that at 480 Hz to determine the circular polarization ρ of the photoluminescence defined as

$$\rho = \frac{I_{PL}(+) - I_{PL}(-)}{I_{PL}(+) + I_{PL}(-)} . \quad (1)$$

With the OPO, the linearly polarized incident light pulses, ~0.4 μsec in duration, were sent through a 60-Hz electro-optic modulator driven by a sine wave whose amplitude was adjusted for a maximum retardation of $\pm\lambda/4$. The OPO was operated at ~40 Hz so that each successive input pulse was shifted by $\sim\frac{3}{2}$ cycles of the 60-Hz modulation. Gated detection of the photoluminescence at the OPO pulse rate, therefore, gives the average signal generated, for + or − inputs, linear (L) inputs, or whatever, depending on the exact phase of the OPO pulses with respect to the modulator voltage. This signal was ratioed with that from a monitor placed downstream from the modulator to yield the average photoluminescence level. Spin-dependent recombination,[7,8] i.e., $[I_{PL}(\pm) - I_{PL}(L)]/I_{PL}(L)$, of a few percent or more is easily detected with this system but was not present in the sample studied herein.

The photoluminescence signal at exactly one-half the OPO repetition frequency (~20 Hz) was also detected, averaged, and ratioed with the average photoluminescence signal at the pulse repetition frequency. When the ~20-Hz photoluminescence pulses are in phase with the + or − voltage peaks of the modulator voltage, this ratioed signal is $I_{PL}(\pm)/\frac{1}{2}[I_{PL}(+) + I_{PL}(-)]$. The deviation of this ratioed signal from unity is the photoluminescence polarization

$$\rho = \frac{I_{PL}(\pm)}{\frac{1}{2}[I_{PL}(+) + I_{PL}(-)]} - 1 = \frac{I_{PL}(+) - I_{PL}(-)}{I_{PL}(+) + I_{PL}(-)} . \quad (2)$$

Therefore, in this mode of operation the OPO repetition frequency is accurately adjusted so that the modulator peak voltage and OPO pulses are in phase once about every 30 seconds. Thus the magnitude of ρ can be determined from the amplitude of the swings of the ratioed signal as a function time. For some experiments, a calcite element was used to produce a circular input polarization constant in time.

The samples were mounted in a variable-temperature cryostat. Provisions were also made to apply a magnetic field B up to about 4.5 kG transverse to the incident light propagation direction (Voigt geometry) for Hanle measurements,[4] i.e., $\rho(B)$.

RESULTS

Figure 1 shows part of the excitation spectrum of the peak photoluminescence intensity using the OPO for excitation with about 60 W/cm^2. These data were taken at 7 K where the peak of the photoluminescence spectrum is at 1.519 eV (8162 Å). For this run, the input and output circular polarizations were kept constant in time and both the same, thereby enhancing the signals for the heavy-hole transitions.[2] All but two of the peaks in the spectrum represent allowed two-dimensional free exciton transitions between hole and electron states each identified with the same quantum number n for the steps in the two-dimensional density of states function.[1] The allowed transitions are identified by E_{nm}, where m signifies whether the transition involves a light or heavy hole, l or h, respectively. In these multilayer structures, the light and heavy holes are split due to the potential well for the valence band.[1] The E_{1h} and E_{1l} transitions can no longer be resolved for pump intensi-

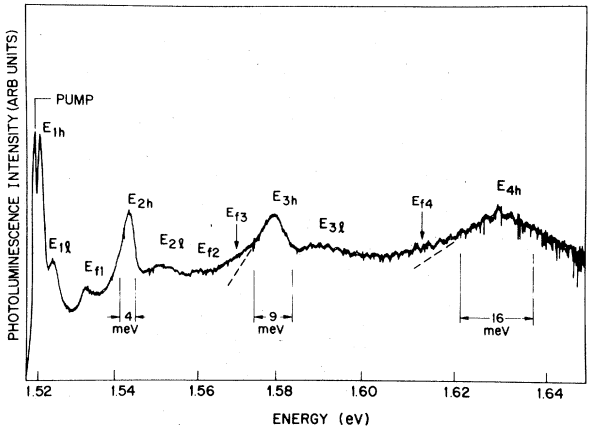

FIG. 1. Excitation spectrum for the multilayer structure showing four allowed heavy-hole exciton transitions and three allowed light-hole exciton transitions, identified by E_{nh} and E_{nl}, respectively. Two forbidden transitions E_{f1} and E_{f2} are also observed as peaks, two others E_{f3} and E_{f4} as shoulders. Widths in meV for the E_{nh} transitions according to Eq. (16) in the text are indicated. Detection was at a photon energy indicated by "pump" in the figure where there is a peak due to scattered pump light.

ties $\gtrsim 1.5$ kW/cm^2 at 7 K. Two forbidden exciton transitions[1] labeled E_{f1} and E_{f2} are also clearly evident in Fig. 1. For these transitions the quantum number n is not the same for the electron and hole. The oscillations in the photoluminescence with a period of ~2 meV at energies $\gtrsim 1.59$ eV are instrumental and result from less than perfect ratioing of the signal and monitor. Exciton transitions E_{5h} and E_{6h} have also been observed with this sample. The excitation spectrum in Fig. 1 demonstrates that the Stokes shift of the photoluminescence peak is quite small, ~1–2 meV. Also, the photoluminescence intensity is unusually bright for a multilayer sample and its width more narrow than usual, ~3 meV at the lowest temperatures. This is therefore, a high quality crystal.

Most of the measurements have been made with the Kr^+ laser, which places the excitation energy, 1.647 eV, between the E_{4h} and E_{5h} transitions where there is little pronounced excitonic structure such as that shown in Fig. 1 at the lower pump photon energies. The photoluminescence signal, and its polarization where possible, have been obtained as a function of wavelength over the temperature range ~6 to ~300 K. At the lowest temperatures, essentially all the emission involves the $n=1$ electron level E_{1e} and the $n=1$ heavy-hole level E_{1hh}. This indicates thermalization of the momentum and energy of the carriers. However, as T is increased, other levels, especially the higher-hole levels, are thermally populated so that additional exciton transitions can be identified in emission. The electron-spin polarization is sometimes useful in identifying these transitions since light- and heavy-hole transitions have opposite polarization. An example of this is shown in Fig. 2 which gives $I_{PL}(\lambda)$ and $\rho(\lambda)$ for $T=87.1$ K. The $I_{PL}(\lambda)$ data show the main peak E_{1h} at 1.511 eV (8205 Å), and shoulders of unresolved peaks at 1.515 eV (8183 Å) and 1.522 eV (8142 Å). The decrease in ρ at 1.515 eV helps confirm that this shoulder is the E_{1l} transition and the ρ increase at 1.522 eV is consistent with the forbidden transition E_{f1} between electron and hole states E_{1e} and E_{3hh}, respectively. A more dramatic example of this method for identifying transitions is shown in Ref. 3. The energies of five different transitions observed in this manner in emission are summarized in Fig. 3. As the temperature is increased, transitions E_{nm} first appear discernibly in emission when the temperature reaches $2kT \gtrsim E_{nm} - E_{1h}$.

Figure 4 shows the full width at half maximum (FWHM) in meV of the photoluminescence spectrum as a function of temperature. The data were obtained with a pump intensity of a few watts per square centimeter using the Kr^+ laser. It appears that inhomogeneous broadening dominates at the

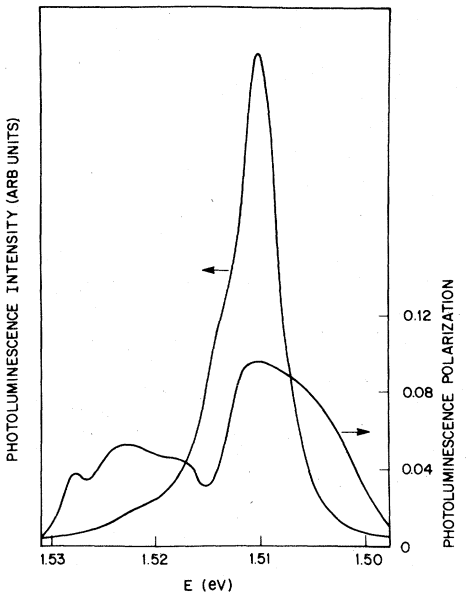

FIG. 2. Photoluminescent intensity and circular polarization versus photon energy at 87 K with excitation at 1.647 eV. Emission at E_{1l} and E_{f1} appear as shoulders on the high-energy side of the peak. The polarization is significantly reduced by the light-hole emission and increases again at the forbidden transition.

lowest temperatures. The point at 195 K is higher than an extrapolation of the lower-temperature data would suggest and is probably due, at least in part, to increased contributions to the photoluminescence from transitions higher in energy than E_{1h}, e.g., E_{2h}. A least-squares fit to all the data points in the figure gives $\Delta E_{1/2}$ (meV) $= 2.66 + 3.5 \times 10^{-2} T$. A broadening linear in kT would give a slope of 8.6×10^{-2} meV/K. The width (FWHM) of

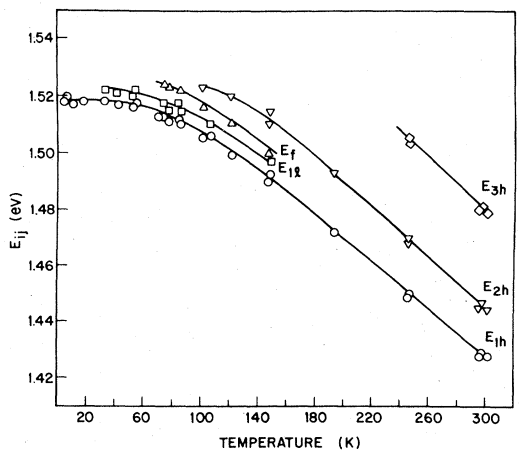

FIG. 3. Various transitions identified in emission as a function of the sample temperature for excitation at 1.647 eV.

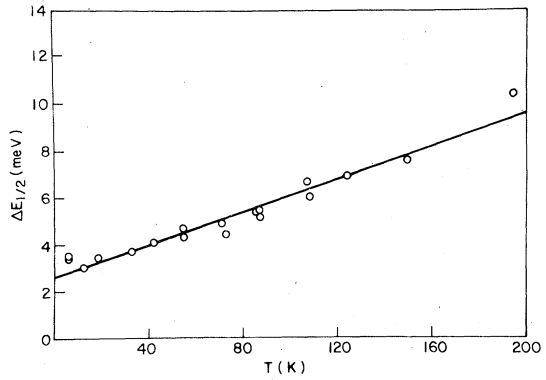

FIG. 4. Full width in meV at half-maximum intensity (FWHM) of the photoluminescence as a function of temperature. The straight line is a least-squares fit to the data.

the E_{1h} transition as observed in the excitation spectrum is about 3 meV, hence in agreement with that observed in the photoluminescence.

The photoluminescence spectrum at 7 K has been measured as a function of the pump intensity I_p from 0.15 to 20 W/cm^2 with the Kr$^+$ laser at 1.647 eV. The logarithm of the integrated photoluminescence intensity

$$W_\lambda = \int_0^{+\infty} I_{\mathrm{PL}}(\lambda) d\lambda , \tag{3}$$

which is approximated by the peak photoluminescence signal times the full width of the spectrum at one-half the peak signal (FWHM), namely, $W_\lambda = I_{\mathrm{PL}}(\mathrm{peak}) \times \mathrm{FWHM}$, is shown versus $\log I_p$ in Fig. 5. A least-squares fit to the data is shown by the solid line which has a slope of 1.00. This again is unusual in that most similar structures examined previously[8] exhibit slopes greater than unity, which causes difficulties when one attempts to generate a simple model to explain the data. Similar data at 50 and 150 K obtained over the same range of I_p as that shown in Fig. 5 give $W_\lambda \propto (I_p)^a$ with $a = 1.08$ and 1.21, respectively. In addition, the OPO was used to obtain $W_\lambda(I_p)$ at 7 K for pump photon energies E_p of 1.519 eV ($a = 0.95$), 1.546 eV ($a = 1.00$). The value of $E_p = 1.519$ eV represents resonant excitation of the E_{1h} transition.

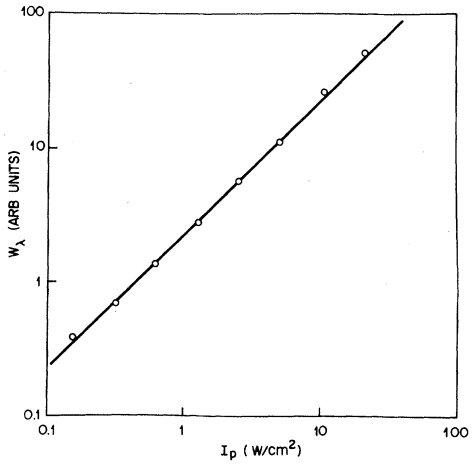

FIG. 5. log of the integrated photoluminescent intensity approximated by the FWHM times the peak intensity versus log of the pump intensity. These data were taken at 7 K with excitation at 1.647 eV. The straight line least-squares fit to the data has a slope of 1.00.

The photoluminescence spectra were also integrated over λ with a planimeter to determine W_λ versus temperature. The results are shown in Fig. 6. The decrease in W_λ between 7 and 196 K is about a factor of 10, which is considerably less than that usually observed with quantum well structures.

With sufficiently intense optical pumping using the OPO and samples ~1 mm long with cleaved facets (mirrors), lasing can be achieved. However, we have only been able to obtain lasing on the E_{1h} transition at both low and high temperatures. In these experiments only the GaAs wells were pumped.

Hanle data[4] on the photoluminescence polarization have been obtained as a function of temperature and pump intensity. These data were taken at the peaks of the photoluminescence spectra and have been analyzed to determine the Hanle time T_1, the electron lifetime τ, and the electron-spin-relaxation time τ_s from the relations[4]

$$\rho(0) = \rho_0(0)/(1+\tau/\tau_s) , \tag{4}$$

and

$$\rho(B)^{-1} = \rho(0)^{-1}[1 + (\gamma T_1 B)^2], \tag{5}$$

with the Hanle time T_1 given by

$$T_1^{-1} = \tau^{-1} + \tau_s^{-1} , \tag{6}$$

and

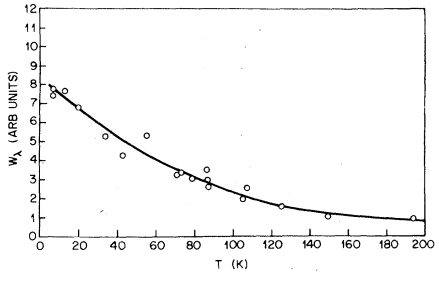

FIG. 6. Logarithm of the integrated photoluminescent intensity W_λ versus temperature for excitation at 1.647 eV. The decrease of W_λ with T is less than that usually observed with multilayer structures.

$$\gamma = |g^*|\mu_B/\hbar = 3.87\times 10^6\ \mathrm{G^{-1}\,sec^{-1}}, \quad (7)$$

based on $g^* = -0.44$ for electrons in GaAs.[9] The quantity $\rho_0(0)$ is the maximum theoretical photoluminescence polarization in the absence of relaxation. It has been assumed that the emission in the temperature range of most interest involves $n=1$ heavy holes, as for example in Fig. 2, which are unpolarized. Also, the valence-band contribution to the excitation with the Kr^+ laser is taken to be the same as for bulk GaAs so that for this multilayer sample $\rho_0(0)=0.50$. The value T_1 is independent of this assumption. Some typical Hanle data taken at several different temperatures are shown in Fig. 7 in terms of $\rho(B)^{-1}$ vs B^2. It is important to note that these data do indeed give linear plots of $\rho(B)^{-1}$ vs B^2 which shows that ρ is Lorentzian in B as required to obtain meaningful times.[4] Actually, very few multilayer samples studied have shown linear $\rho(B)^{-1}$ vs B^2 plots. In fact, even with bulk material, we generally observe linear plots only when the material is heavily doped p type, e.g., $[\mathrm{Zn}] \gtrsim 10^{18}\ \mathrm{cm^{-3}}$.

Figure 8 shows a plot of $\rho(0)^{-1}$ and T_1 versus temperature. The Hanle time goes through a maximum at ~70 K while $\rho(0)^{-1}$ continues to increase with temperature. The equivalent data for τ and τ_s are given in Fig. 9. There is a fair amount of scatter in the τ data so that the points for $T>50$ K were fitted via a least-squares analysis. Whereas τ increases with T over the range measured, τ_s goes through a maximum at about 60 K.

The pump intensity dependences of τ and τ_s were also determined via Hanle runs. Over the same excitation intensity range as that shown in Fig. 5,

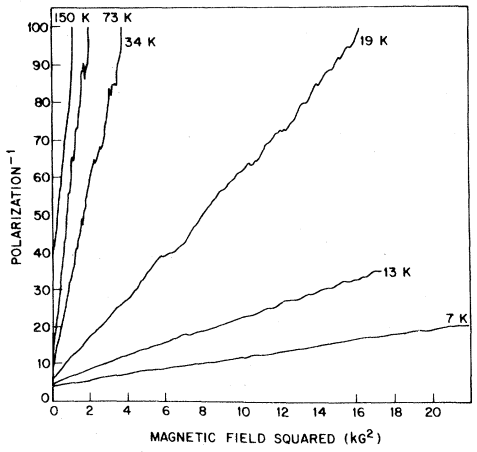

FIG. 7. Typical Hanle plots for several temperatures of the reciprocal of the circular polarization versus the magnetic field squared. The values of the slopes and intercepts are used to determine the electron-spin-relaxation time and electron lifetime.

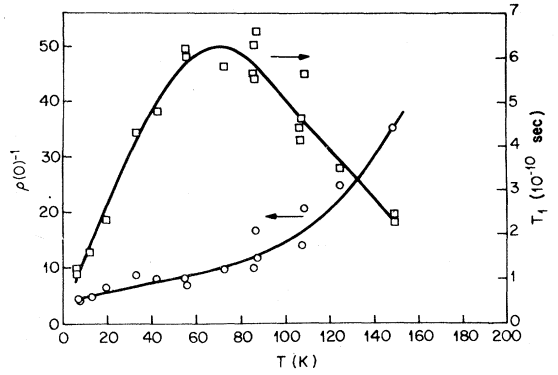

FIG. 8. Hanle time and photoluminescent circular polarization versus sample temperature.

the I_p dependence of τ and τ_s at 7 K in units of 10^{-10} sec can be described by $2.37+0.16\ \log I_p$ and $2.10+0.35\ \log I_p$, respectively, with I_p in $\mathrm{W/cm^2}$. However, at 50 and 150 K, both τ and τ_s were, within the experimental uncertainties, essentially independent of I_p over the range studied. Thus the variation of these times with I_p is relatively small.

REDUCTION OF DATA

Several aspects of the reduction of the raw data require some comment. First of all, in determining τ and τ_s it has been assumed that the emission observed at the peak of the photoluminescence involves only the $n=1$ heavy hole, i.e., $\rho_0(0)$ in Eq. (5) $=0.5$. Examination of the photoluminescence spectra shows that this is certainly a good approximation below about 90 K where, as can be seen in Fig. 2, the E_{1l} emission peak (shoulder) is shifted from E_{1h} by more than one-half the FWHM energy of the E_{1h} peak. For $T \gtrsim 90$ K, there is undoubtedly some contribution from E_{1l} at the peak photolum-

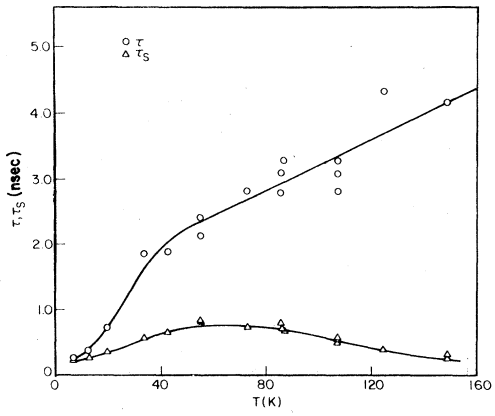

FIG. 9. Electron-spin-relaxation time and lifetime versus sample temperature.

inescence emission. If above 100 K, this contribution is considered to be at its full strength as in bulk GaAs, which is certainly not the case here, $\rho_0(0)=0.25$. The result is then that the calculated values of τ should be halved, and the values of τ_s increased by $\lesssim 20\%$. However, the effects on τ and τ_s due to contributions from E_{1l} emission do not significantly alter the conclusions and interpretations given herein.

Another point that requires comment is that at low temperatures the emission arises from the recombination of free excitons. In fact, the various peaks in Fig. 1 show that excitation can involve the generation of free excitons. This has prompted a search in this sample and other multilayer structures for optical alignment[6] effects which require a coherence between the electron and hole in the generated excitons that is retained until radiative recombination occurs. Optical alignment effects, for example, produce linearly polarized photoluminescence from linearly polarized excitation. Attempts to observe this effect in this sample and other multilayer samples were without success. Any linear polarization in the photoluminescene, if present, must be less than a few percent. The absence of optical alignment and the straight $\rho(B)^{-1}$ vs B^2 plots (Fig. 7) both argue against significant hole polarization under the present experimental conditions. Hole polarization might have been expected here at low temperatures since the light and heavy holes are split by the well potential.

For the analyses of the Hanle runs the hole polarization was taken as zero and the g^* factor employed was that for free electrons in GaAs, namely -0.44.[9] However, since the g^* factor for $n=1$ heavy holes in this type structure is zero,[6] and the e-h exchange energy is very small, ~0.1 meV,[10] $g^*=-0.44$ would seem appropriate for both free electrons and excitons. The Hanle time T_1, τ, τ_s are all proportional to $|g^*|^{-1}$.

DISCUSSION

Since the data in Fig. 5 and other data discussed above demonstrate that to a good approximation $W_\lambda \propto I_p^{1.0}$, it is proposed that the differential equation describing the number of optically excited excitons N_x can be described by

$$\frac{dN_x}{dt}=g-\frac{N_x}{\tau}, \tag{8}$$

where g is the generation rate, a linear function of I_p, and τ is the lifetime. The steady-state solution is $N_x=g\tau$ so that the photoluminescence can be described by

$$W_\lambda \propto N_x/\tau_r = g\tau/\tau_r, \tag{9}$$

where τ_r is the radiative lifetime and

$$\tau^{-1}=\tau_r^{-1}+\tau_n^{-1}. \tag{10}$$

In Eq. (10), τ_n is the nonradiative lifetime for the excitons. The internal quantum efficiency $\eta_i=\tau/\tau_r$. Hence for constant g, an assumption which will be discussed later, η_i is proportional to W_λ. Therefore, the data in Fig. 6 show that η_i drops by an order of magnitude between 7 and 200 K.

Equation (9) suggests that a plot of $g\tau/W_\lambda \propto \tau_r$ vs T would give the temperature dependence of τ_r. This calculation has been made and the result is shown plotted as $\log\tau/W_\lambda$ vs $\log T$ in Fig. 10. A least-squares straight line fit to the data is shown in the figure and gives $\tau_r \propto T^{1.51}$. As discussed above, contributions to the photoluminescence from E_{1l} transitions could somewhat reduce the values of τ above ~100 K. However, all the data up to about 100 K are well described by $\tau_r \propto T^{1.51}$. This temperature dependence for τ_r, nominally $T^{3/2}$, is that calculated for band-to-band transitions obeying k conservation in bulk direct band-gap III–V compounds.[11] It should be noted that the same picture with two-dimensional k conservation in the plane of the wells would predict a linear T dependence.

For a multilayer structure, k conservation would apply only in two dimensions and would lead to a linear T dependence at sufficiently low temperatures that the occupation of the higher-hole

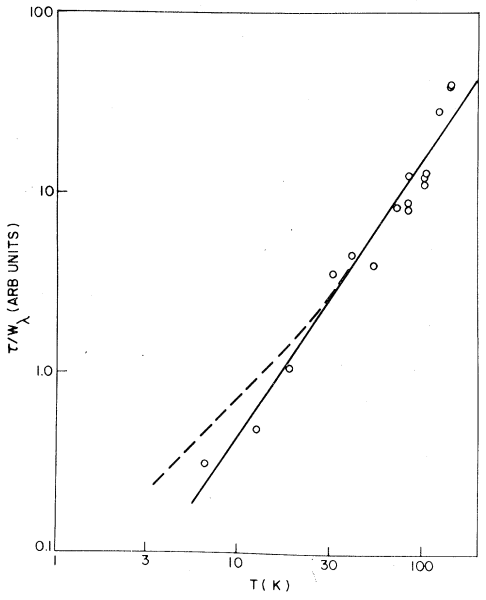

FIG. 10. Logarithm of the electron lifetime divided by the integrated photoluminescent intensity, which is proportional to the radiative lifetime, versus $\log T$. The straight line least-squares fit has a slope of 1.5. The theoretical relation given by Eq. (12) is shown dashed.

levels is negligible. If the radiation is predominantly due to excitons, k conservation requires that only excitons of total $k=0$ can radiate, and again leads to a linear T dependence at low temperature. However, with increasing T thermal excitation to higher-hole levels will lead to a dependence approximately of the form

$$\tau_r \propto T \sum_{n,m} \exp[-(E_{nmh} - E_{1hh})/kT], \tag{11}$$

where E_{nmh} denotes the possible hole energies in the quantum well. This relation is shown (dashed curve) in Fig. 10 with one adjustable parameter chosen to give agreement at 100 K with the least-squares line.

For the purpose of this calculation Eq. (11) was approximated by the formula

$$\tau_r \propto T \sum_{n=1}^{\infty} \exp[-(n^2-1)E_{1hh}/kT], \tag{12}$$

with $E_{1hh}=1.0$ meV, the ground state for $m_{hh}=0.45m_e$ in a well high enough to bind 6 levels. The justification for Eq. (12), which appears to neglect the lh levels is that the $1lh$ level, can be regarded as a radiating level included in W_λ, and the higher lh levels can be lumped together with a nearby hh level. In fact, precise values of E_{nmh} are not required in Eq. (11) in the temperature region of interest because the sum extends over a number of terms and the spectrum of Fig. 1 indicates considerable broadening of the higher levels.

Equations (9) and (10) can also be written in the form

$$W_\lambda \propto (1 - \tau/\tau_n)g. \tag{13}$$

Thus it appears that it might be useful to plot W_λ vs τ as is done in Fig. 11. The straight line in the figure is a least-squares fit to the data and suggests that both g and τ_n do not change significantly over the range of τ, i.e., T, measured. These data, therefore, support the assumption made earlier that g is essentially independent of T. The slope in Fig. 11 gives $\tau_n = 4.9\times10^{-9}$ sec. The magnitude of the radiative lifetime can now be calculated as a function of T from Eq. (10) making use of the data (or fitted curve) on $\tau(T)$ shown in Fig. 9. The result, which is consistent with Fig. 10, can be represented by $\tau_r(T) = 1.1\times10^{-11}T^{3/2}$ sec. At ~7 K, $\tau_r = 2.7\times10^{-10}$ sec, indicating an internal quantum efficiency $\eta_i = 0.95$ which drops off to about 0.1 at ~150 K.

The temperature dependence of τ_s is also of interest since it may shed some light on the mechanism for electron-spin relaxation.[10] A plot of $\log\tau_s$ vs $\log T$ is given in Fig. 12. These data are quite similar to those obtained earlier by Clark *et al.* for p-type bulk $Al_xGa_{1-x}As$, who found that τ_s increases with T at low temperatures, i.e., $T<50$ K, and then decreases as T^{-b} in the high-temperature region with b in the range 1.8 to 3.3 for the six samples studied.[12] More recently, Clark *et al.*[13] have measured GaAs doped with $[Zn]\sim10^{17}$ cm^{-3} and found a gradual dropoff in τ_s vs T for $T<40$ K and $\tau_s \propto T^{-1.3}$ for higher temperatures. Some representative data from this work are also shown in Fig. 12. Fishman and Lampel (FL) have measured τ_s in bulk GaAs doped with $[Zn]\sim4\times10^{18}$ cm^{-3} from ~2 to ~90 K.[10] Over this range their data can be fit by $\tau_s = 3.5\times10^{-10}\,T^{-1/2}$ sec. Part of their data is also shown in Fig. 12.

The work by Clark *et al.*, as well as the present work, suggests different relaxation mechanisms in the low- and high-temperature regions. The

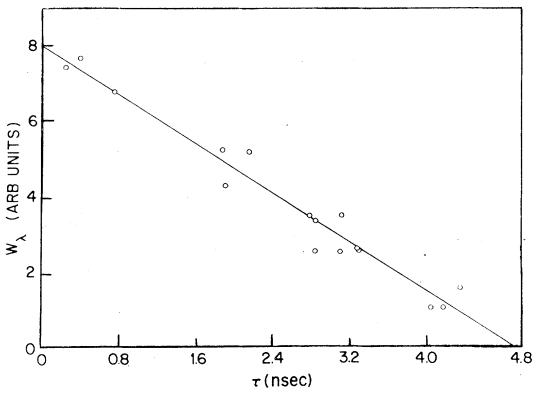

FIG. 11. Integrated photoluminescence versus the electron lifetime. Temperature increases to the right as can be seen from Fig. 9. The slope of the least-squares fit leads to a nonradiative lifetime of 4.9×10^{-9} sec.

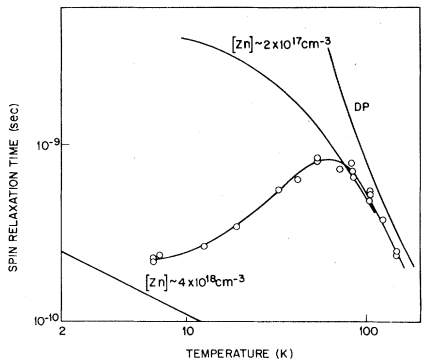

FIG. 12. Plot of the spin-relaxation time versus temperature. Also shown are data from Clark *et al.* (Ref. 13) on bulk GaAs doped with $[Zn]\sim2\times10^{17}$ cm^{-3} and Fishman and Lampel data[10] for $[Zn]\sim4\times10^{18}$ cm^{-3}. Estimates of τ_s for the D'yakonov-Perel' (DP) process are in good agreement with the high-temperature multilayer τ_s data.

multilayer data on τ_s shown in Fig. 9 suggest that there is some shallow center with a binding energy of ~5 meV which relaxes the spin. As the temperature is increased the electrons spend less and less time in the vicinity of the center such that at ~60 K, another relaxation process dominates. The authors have not been able to identify this center.

The e-h exchange mechanism seems to describe satisfactorily the FL (Ref. 10) data and the low-temperature Clark *et al.* data.[10,13] This mechanism is not relevant in the present case, since there are essentially no equilibrium holes present and few nonequilibrium holes. On the other hand, the high-temperature results of Clark *et al.* are attributed[10,13] to the D'yakonov-Perel' (DP) process.[5] In the DP process, a precession of the electron spin occurs due to a pseudo-magnetic-field $\propto k^3$ caused by a lack of inversion symmetry and spin-orbit coupling. This mechanism is estimated for bulk material to give[13]

$$\tau_s = 5 \times 10^{-16}/(\tau_p T^3) , \tag{14}$$

where τ_p is the momentum relaxation time. This relation should apply to a multilayer at temperatures $kT > 2E_{1e}$ corresponding to $T > 150$ K in the present case; at lower temperatures one expects $\tau_s \propto 1/(\tau_p T)$ when motion of the electrons is confined to the plane of the layers.

According to FL,[10] another spin-relaxation mechanism likely to be relevant in the high-temperature region is the Elliott-Yafet[14,15] (EY) process. The EY mechanism leads to spin relaxation due to an admixture of the valence-band states into the conduction band for $k \neq 0$. Thus momentum scattering can produce a spin flip. Clark *et al.*[13] estimate for bulk GaAs that this mechanism gives

$$\tau_s = 2 \times 10^9 \tau_p / T^2 . \tag{15}$$

Using the high-temperature electron mobility data of Dingle *et al.*[16] for undoped quantum wells and ignoring screening effects, $\tau_p(T)$ has been estimated assuming that the time extracted from the mobility is indeed τ_p. Then τ_s can be estimated from Eqs. (14) and (15) and the results for the DP process are shown in Fig. 12. The values of τ_s estimated from Eq. (15) are too large by more than an order of magnitude, while those obtained from Eq. (14) give a good fit to the quantum-well high-temperature data. We therefore tentatively conclude that the DP mechanism is the relevant one for this multilayer structure in the high-temperature region as in the earlier work on bulk GaAs by Clark *et al.*[13]

An interesting feature of Fig. 1 is the broadening that increases dramatically in going from E_{1h} to E_{4h}. This broadening is consistent with the simple relation

$$\Delta E_n = \Delta E_1 \times n^2 , \tag{16}$$

with $\Delta E_1 \sim 1.0$ meV. The widths given by Eq. (16) are indicated in Fig. 1. Also indicated are dashed lines on E_{3h} and E_{4h} extending the low-energy sides of these peaks. This construction reveals additional forbidden transitions E_{f3} and E_{f4} indicated by arrows in Fig. 1. The broadening given by Eq. (16) is what would be expected from a nonconstant layer width of the GaAs wells with a spread (FWHM) $\Delta l \sim l/13 = 20$ Å. The spread in Δl estimated from the known MBE growth parameters is 14 Å. The width $\Delta E_1 \sim 1$ meV is consistent with the inhomogeneous width 2.7 meV obtained from the least-squares fit to the data in Fig. 4. About 1.7 meV of inhomogeneous broadening of the photoluminescence must therefore be attributed to such sources as variations of composition, impurity concentration, or strains.

All of the "forbidden" transitions can be given reasonable assignments as follows:

$$\begin{aligned} f_1 &= (1e, 3hh) , \\ f_2 &= (2e, 4hh) , \\ f_3 &= (3e, 1hh) , \\ f_4 &= (4e, 2hh) . \end{aligned} \tag{17}$$

It is recognized that the general features of multilayer photoluminescence spectra can be understood[1] in terms of (a) the quantum levels of electrons and holes confined in one dimension to a potential well and (b) the formation of excitons in the other two dimensions. Computer studies are currently under way on this sample and others to determine how precisely this model can explain the multilayer spectra. Details of these calculations will not be discussed here, but preliminary results confirm the reasonableness of Eqs. (17). One would expect forbidden transitions to be observable as a result of curvature of the bottom of the potential well due to the transfer of holes or electrons from the barriers into the wells. The curvature would be symmetric about the well center and, therefore, would only couple electron and hole states of the same parity. Thus one would not expect, for example, to see the transitions $(1e, 2hh)$ or $(1e, 4hh)$. Furthermore, since the matrix element is essentially the same for $(1e, 3hh)$ and $(3e, 1hh)$, one would expect to see both or neither, but not one without the other.

CONCLUSIONS

Studies of various aspects of the photoluminescence of a high-quality multilayer crystal have led to a more complete understanding of such struc-

tures. An examination of the heavy-hole exciton transitions in the excitation spectrum of the photoluminescence leads to the conclusion that these transitions are broadened due to the spread in the GaAs well widths. Four forbidden transitions are identified and ascribed to parity-conserving electron-to-heavy-hole transitions. Five transitions have been seen in spontaneous emission. However, we have observed stimulated emission only on the lowest-energy transition which involves the $n=1$ electron and heavy hole.

The temperature dependence of the electron-spin-relaxation time τ_s, determined from the Hanle effect, suggests that there is a center with a binding energy of ~5 meV that relaxes the electron spin. At higher temperatures the electron-spin relaxation is believed due to the D'yakonov-Perel' mechanism[5] and the values observed are close to earlier results obtained by others for bulk p-type GaAs, $[\mathrm{Zn}] \sim 10^{17}$ cm^{-3}.[13]

The linear Hanle plots of the reciprocal of the photoluminescence polarization versus the magnetic field squared and the absence of optical alignment[6] when exciting with linearly polarized light both suggest that no hole polarization is present even though the light and heavy-hole energies are split by the potential.

The linear dependence of the photoluminescence on the excitation intensity and on the observed electron lifetime (Fig. 11) leads to a simple model from which the nonradiative lifetime is found to be nearly constant and equal to $\sim 5 \times 10^{-9}$ sec. The calculated values of the radiative lifetime are estimated to be as short as $\sim 3 \times 10^{-10}$ sec at 7 K and indicate a very high quantum efficiency at low temperatures. The observed temperature dependence of the radiative lifetime is in agreement with expectations for a two-dimensional system when the thermal excitation of holes is taken into account.

ACKNOWLEDGMENT

The authors would like to thank Dr. Claude Weisbuch for numerous fruitful discussions on the subject of this paper.

[1]R. Dingle, in *Festkorperprobleme*, Advances in Solid State Physics, edited by H. J. Queisser (Pergamon/Vieweg, Braunschweig, 1975), Vol. XV, p. 21.

[2]R. C. Miller, D. A. Kleinman, and A. C. Gossard, in *Proceedings of the Fourteenth International Conference on the Semiconductors, Edinburgh, 1978*, edited by B. L. H. Wilson (Institute of Physics, London, 1979), p. 1043.

[3]C. Weisbuch, R. C. Miller, R. Dingle, and A. C. Gossard (unpublished).

[4]R. R. Parsons, Phys. Rev. Lett. 23, 1152 (1969).

[5]M. I. D'yakonov and V. I. Perel', Zh. Eksp. Teor. Fiz. 65, 362 (1973) [Sov. Phys.—JETP 38, 177 (1974)].

[6]E. F. Gross, A. K. Ekimov, B. S. Razbirin, and V. I. Safarov, Pis'ma Zh. Eksp. Teor. Fiz. 14, 108 (1971) [JETP Lett. 14, 70 (1971)].

[7]C. Weisbuch and G. Lampel, Solid State Commun. 14, 141 (1974).

[8]R. C. Miller, W. T. Tsang, and W. A. Nordland, Jr., Phys. Rev. B 21, 1569 (1980).

[9]C. Weisbuch and C. Hermann, Phys. Rev. B 15, 816 (1977).

[10]G. Fishman and G. Lampel, Phys. Rev. 16, 820 (1977).

[11]V. H. Barry Bebb and E. W. Williams, in *Semiconductors and Semimetals*, edited by R. K. Willardson and A. C. Beer (Academic, New York, 1972), Vol. 8, p. 239.

[12]A. H. Clark, R. D. Burnham, D. J. Chadi, and R. M. White, Phys. Rev. B 12, 5758 (1975).

[13]A. H. Clark, R. D. Burnham, D. J. Chadi, and R. M. White, Solid State Commun. 20, 385 (1976).

[14]R. J. Elliott, Phys. Rev. 96, 266 (1954).

[15]Y. Yafet, in *Solid State Physics*, edited by F. Seitz and D. Turnbull (Academic, New York, 1963), Vol. 14, pp. 1–98.

[16]R. Dingle, H. L. Störmer, A. C. Gossard, and W. Wiegmann, in *Proceedings of the Fourteenth International Conference on the Physics of Semiconductors, Edinburgh, 1978*, edited by B. L. H. Wilson (Institute of Physics, London, 1979), p. 557.